



Radomir Jovičić¹, Simon Sedmak¹, Nada Ilić², Ljubica Radović², Svetlana Štrbački³, Milica Antić⁴, Zijah Burzić²

UTICAJ TEMPERATURE IVICE ŽLJEBA I UNETE TOPLOTE NA STRUKTURU I TVRDOĆU ZONE UTICAJA TOPLOTE ZAVARENOG SPOJA ČELIKA P 460 NL1

THE IMPACT OF GROOVE EDGE TEMPERATURE AND HEAT INPUT ON THE STRUCTURE AND HARDNESS OF THE HEAT AFFECTED ZONE OF STEEL 460 NL1 WELDED JOINT

Originalni naučni rad / Original scientific paper

Rad je u izvornom obliku objavljen u Zborniku sa 4. IIW Kongresa zavarivanja Jugoistočne Evrope „Safe Welded Construction by High Quality Welding“ održanog u Beogradu 10-13. Oktobra 2018

Rad primljen / Paper received:

Jul 2018.

Ključne reči: temperatura ivice žleba, vreme hlađenja $t_{8/5}$, strukture, tvrdoće

Abstrakt

Polazne strukture i vreme hlađenja u temperaturnom intervalu 800 - 500°C ($t_{8/5}$) imaju presudan uticaj na strukture i osobine zone uticaja toplote zavarenih spojeva čelika. Na vreme hlađenja $t_{8/5}$ između ostalog, utiče i temperatura ivice žleba. Zbog zagrevanja toplotom luka temperatura ivice žleba duž spoja raste, zbog čega se vreme hlađenja zone uticaja toplote produžava. Samim tim, duž spoja se produžava i vreme hlađenja $t_{8/5}$. U radu su prikazani rezultati merenja temperatura ivica žleba pri zavarivanju višeprolaznog sučeonog spoja mikrolegiranog čelika P 460 NL1. Određen je uticaj ovih temperatura na vremena hlađenja $t_{8/5}$ i na makro i mikrostrukture i tvrdoće u zoni uticaja toplote ovog zavarenog spoja.

1.Uvod

Odlučujući uticaj na dobijene strukture u zoni uticaja toplote (ZUT) čelika imaju njegov hemijski sastav, polazna struktura i vreme hlađenja u temperaturnom intervalu najmanje stabilnosti austenita tj. u temperaturnom intervalu 800 – 500°C. Na vreme hlađenja ZUT imaju uticaj fizičke osobine čelika, toplotna provodljivost i specifična toplota, debљina osnovnog materijala (OM), tip spoja i parametri zavarivanja, tj. temperatura OM i količina unete toplote. Sniženje temperature OM uz ivicu žleba ubrzava hlađenje ZUT i skraćuje vreme $t_{8/5}$. Zbog toga se, u ZUT, povećava sklonost ka obrazovanju struktura koje su sklone zakaljivanju, otežava se oslobođanje gasova iz MŠ, čime se povećava verovatnoća pojave poroznosti i povećava količina rastvorenih gasova u MŠ i ZUT,

Adresa autora / Author's address:

¹Inovacioni centar Mašinskog fakulteta Univerziteta u Beogradu, Srbija

²Vojno – tehnički institut, Beograd, Srbija

³KonMat doo, Beograd, Srbija

⁴Društvo za unapređenje zavarivanja u Srbiji, Beograd, Srbija

Key words: groove edge temperature, cooling time $t_{8/5}$, structure, hardness

Abstract

The starting structures and cooling times in the temperature range 800 - 500°C ($t_{8/5}$) have a decisive influence on the structures and properties of the heat affected zone of steel welded joints. At the cooling time $t_{8/5}$, inter alia, the groove edge temperature has an effect. Due to heating by the electrical arc, the groove edge temperature along the joint, increases, resulting in extending of the cooling time of the heat affected zone. Therefore, the cooling time $t_{8/5}$ is extended along the joint. The paper presents the measurement results of the groove edges temperature during the welding of the multilayer joint of the microalloyed steel P 460 NL1. The influence of these temperatures on the cooling time $t_{8/5}$ and on the macro and microstructure and hardness in the heat affected zone of this welded joint was determined.

1. Introduction

The decisive influence on the obtained structures in the heat-affected zone (HAZ) of steel has its chemical composition, the starting structure and the cooling time in the temperature interval of at least the austenite stability, i.e. in a temperature range of 800-500 °C. At the HAZ cooling time, influences physical properties of the steel, the thermal conductivity and the specific heat, the thickness of the base material (BM), the type of joints and the welding parameters, i.e. BM temperature and amount of heat input. Lowering the BM temperature along the groove edge accelerates the cooling of the HAZ and shortens the time $t_{8/5}$. Therefore, in the HAZ, the possibility to form structures that are prone to quenching increases, the release of gases from the WM is complicated, which što je



naročito važno kada je u pitanju vodonik. Takođe, zbog povećanja temperaturnog gradijenta, povećavaju se zaostali naponi. Sve ovo utiče na povećanje sklonosti zavarenih spojeva ka pojavi hladnih prslina [1, 2]. Povećanje temperature OM uz ivicu žleba dovodi do povećanja udela OM u sastavu MŠ, zatim do širenja ZUT, do širenja krupnozognog dela ZUT i do rasta zrna u ZUT, što ima za posledicu pad mehaničkih osobina u ovom delu spoja [3].

Željene strukture i osobine ZUT, kod zavarivanog čelika, se mogu dobiti samo pri odgovarajućem vremenu hlađenja $t_{8/5}$. Vezu između struktura ZUT i vremena $t_{8/5}$ daju TTT dijagrami izrađeni za uslove zavarivanja. Zadato vreme $t_{8/5}$, za određeni čelik, se postiže unosom odgovarajuće količine toplote (Q) pri određenoj temperaturi ivice žleba. Usled zagrevanja OM topotom luka temperatura ivice žleba i njegove okoline duž spoja raste, zbog čega se vreme $t_{8/5}$, duž spoja produžava. Prema tome, da bi se u realnim uslovima, u ZUT dobiti željene strukture potrebno je odrediti dijapazon vremena hlađenja $t_{8/5}$, koji ima donju i gornju graničnu vrednost [4]. Ovo je naročito važno kada se zavaruju čelici koji se proizvode u uslovima precizno vođenih režima termomehaničke obrade.

2. Vreme hlađenja $t_{8/5}$ i temperatura ivice žleba

Postupak za određivanje vremena hlađenja $t_{8/5}$ je opisan u literaturi [5]. Prvi korak u proračunu je određivanje potrebne temperature predgrevanja (T_p) i međuprolazne temperature (T_{mp}) u uslovima u kojima se zavaruje određeni spoj. U eksperimentalnom delu ovog rada predviđeno je da ispitni spoj bude sučeoni spoj zavaren na čeliku P 460 NL1, debljine 14mm. Hemski sastav korišćene šarže čelika je dat u tabeli 1. Za zavarivanje su odabrani MAG postupak, zaštitni gas mešavina 82% Ar – 18% CO₂ i dodatni materijal (DM) G46 4M/C G4Si1 (EN ISO 14341-A) prečnika 1,2 mm.

which is especially important when it connected to hydrogen. Also, due to an increase in the temperature gradient, the residual stresses increase. All that affects the increase in the tendency of welded joints to the appearance of cold cracks [1,2]. Increasing the BM temperature along the groove edge, leads to an increase in the proportion of BM in the composition of WM, then to the spread of HAZ, to the spread of the coarse-grain part of HAZ and to the grain growth in HAZ, resulting in a drop in mechanical properties in this part of the joint [3]. Preferred structures and properties of HAZ, for welded steel, can be obtained only at the appropriate cooling time $t_{8/5}$. The connection between the HAZ structures and the time $t_{8/5}$ permits TTT diagrams designed for welding conditions. The given time $t_{8/5}$ for certain steel is achieved by the appropriate heat input (Q) at a certain temperature of the groove edge. Due to the heating of the BM by the heat of electrical arc, the temperature of the groove edge and its surroundings along joint is increased, which causes that time $t_{8/5}$ along joint be extended. Therefore, in order to obtain the desired structures in the HAZ, in real terms, it is necessary to determine the slope of cooling time $t_{8/5}$, which has a lower and upper limit value [4]. This is especially important during welding of steels which are produced under the conditions of precisely controlled thermo-mechanical treatment.

2. Cooling time $t_{8/5}$ and groove edge temperature

The procedure for determining the cooling time $t_{8/5}$ is described in the literature [5]. The first step in calculation is to determine the required preheating temperature (T_p) and the interpass temperature (T_i) in the conditions in which a particular joint is welded. In the experimental part of this paper, it is anticipated that the test joint is a welded joint of steel P 460 NL1, thickness of 14 mm. The chemical composition of used steel batch is given in Table 1. For welding process, GMAW process, the protective gas mixture 82% Ar-18% CO₂ and filler material (FM) G46 4M / C G4Si1 (EN ISO 14341-A) with diameter of 1,2 mm are selected.

increases the likelihood of porosity and increases the amount of dissolved gases in the MW and HAZ,

Element	C	Si	Mn	P	S	Al	Cr	Ni
%	0,160	0,390	1,420	0,007	0,003	0,031	0,04	0,670
Element	Mo	Cu	V	Nb	Ti	B	N	-
%	0,008	0,093	0,098	0,038	0,03	0,0003	0,0055	

Table 1. Chemical composition of the base material
Tabela 1. Hemski sastav osnovnog materijala



Jednačine i podaci potrebni za proračun T_p i T_{mp} , kao i njihove izračunate vrednosti za navedeni spoj, su dati u tabeli 2. Parametar CET je izračunat na osnovu jednačine 2 iz tabele 2. i podataka iz tabele 1. Parametar T_{pQ} je izračunat na osnovu očekivanih količina unete toplote za koren i zavar i zavare popune, tabela 3. Količine unete toplote su izračunate iz jednačine 5, tabela 2. i parametara za zavarivanje, tabela 3. Iz tabele 2. se vidi da se parametar T_{pQ} razlikuje za koren i zavare popune, zbog čega se razlikuju T_p i T_{mp} , ali ne značajno.

The equations and data required for T_p and T_i calculation, as well as their calculated values for given joint, are presented in table 2. CET parameter is calculated on the basis of the equation 2 in table 2 and the data in table 1. T_{pQ} parameter is calculated on the basis of the expected heat input for root and other weld runs, table 3. Quantities of heat inputs are calculated from equation 5, table 2 and welding parameters, table 3. From table 2 it can be seen that T_{pQ} parameter is different for the root and other weld runs, and because of that, T_p and T_i differentiate, but not significantly.

		Jednačine	Parametri	Temp. °C
1	T_{pCET}	$T_{pCET} = 750 \cdot CET - 150$		+ 95,3
2	CET	$CET = C + (Mn + Mo)/10 + (Cr + Cu)/20 + Ni/40 (\%)$	$CET = 0,327$	
3	T_{pd}	$T_{pd} = 160 \cdot \tanh(d/35) - 110$	$d = 14 \text{ mm}$	- 49,2
4	T_{pHD}	$T_{pHD} = 62 \cdot HD^{0,35} - 100$	$HD = 5 \text{ ml}/100 \text{ gr}$	+ 8,9
5	Q	$Q = \eta \cdot I \cdot U/(v_z \cdot 1000) [\text{KJ/mm}]$	$\eta = 0,8; I [\text{A}]; U [\text{V}]; v_z [\text{mm/sec}]$	
6	T_{pQ} – koren	$T_{pQ} = (53 \cdot CET - 32) Q - 53 \cdot CET + 32$	$Q = 1,25 \text{ KJ/mm}$	- 3,6
7	T_p - koren	$T_p = T_{pCET} + T_{pd} + T_{pHD} + T_{pQ}$	-	51,4
8	T_{pQ} – popuna	$T_{pQ} = (53 \cdot CET - 32) Q - 53 \cdot CET + 32$	$Q = 1,32 \text{ KJ/mm}$	- 4,7
9	T_p - popuna	$T_p = T_{pCET} + T_{pd} + T_{pHD} + T_{pQ}$	-	50,3

Table 2. Calculation of preheating temperature T_p and interpass temperature T_i
Tabela 2. Propracun temperature predgrevanja T_p i međuprolazne temperature T_{mp}

		T_p °C	I A	U V	v_z cm/min	v_z mm/sec	Q KJ/mm	$t_{8/5}$ sec
1	Root run	51	130	16,0	8,0	1,33	1,25	9,3
2	Filling runs	50	230	30,0	25,0	4,17	1,32	10,3

Table 3. Welding parameters, heat input and cooling time $t_{8/5}$
Tabela 3. Parametri zavarivanja, količine unete toplote i vremena hlađenja $t_{8/5}$

Sledeći korak u određivanju vremena hlađenja $t_{8/5}$ je određivanje prelazne debljine OM. To je debljina OM pri kojoj se odvođenje toplote menja iz dvodimenzionalnog u trodimenzionalno. Za uslove zavarivanja korenog zavara i zavara popune, u razmatranom primeru, prelazna debljina iznosi 18 mm, [5]. S obzirom da je debljina OM manja od prelazne debljine, u konkretnom slučaju se radi o dvodimenzionalnom odvođenju toplote.

Jednačina za određivanje vremena $t_{8/5}$ za niskougljenične i mikrolegirane čelike, pri dvodimenzionalnom odvođenju toplote, [5] glasi:

$$t_{8/5} = (4300 - 4,3 T_p) \cdot 10^5 \cdot Q^2/d^2 \cdot [1/(500 - T_p)^2 - 1/(800 - T_p)^2] \cdot F_2 \text{ sec } (1)$$

gde su: T_p – temperatura predgrevanja °C; Q – količina toplote unete KJ/mm; d – debljina OM mm; F_2 – faktor oblika spoja.

The next step in cooling time $t_{8/5}$ determining is the determination of BM transient thickness. This is BM thickness at which the heat transfer changes from two-dimensional to three-dimensional. For the conditions of root run and filling runs, in the considered case, transient thickness is 18 mm [5]. Since BM thickness is less than the transient thickness, in concrete case it is a two-dimensional heat transfer.

The equation for determining time $t_{8/5}$ for low-carbon and micro-alloyed steels, in the case of two-dimensional heat transfer, [5] is:

$$t_{8/5} = (4300 - 4,3 T_p) \cdot 10^5 \cdot Q^2/d^2 \cdot [1/(500 - T_p)^2 - 1/(800 - T_p)^2] \cdot F_2 \text{ sec } (1)$$

Where: T_p is the preheating temperature °C; Q - heat input KJ/mm; d - BM thickness; F_2 - factor of joint shape.

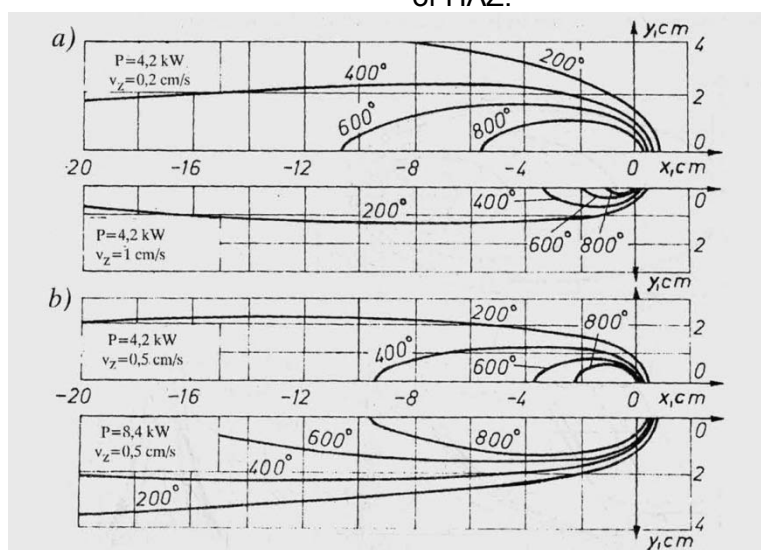


Preporučena vremena hlađenja $t_{8/5}$, za niskougljenične i mikrolegirane čelike u koje spada i čelik P 460 NL1, se kreću u intervalima 10 - 25 sec. [5], 15 sec [6] i 5 - 20 sec. [7]. Razlike u preporučenim vremenima hlađenja su posledica razlika u hemijskim sastavima i mikrostrukturom ispitivanih OM. Za potrebe ovog rada, kao optimalan, usvojen je raspon vremena hlađenja $t_{8/5}$ od 10 do 20 sec. Izračunata vremena $t_{8/5}$, tabela 3. su na donjoj granici optimalnih vrednosti.

Rasprostiranje toplote u OM, pri elektrolučnom zavarivanju, je prikazano na slici 1. [8]. Sa slike se vidi da se raspored temperatura i oblici temperaturnih polja menjaju pri različitim snagama i brzinama kretanja luka. Sa slike se vidi i da se temperatura OM levo i desno i ispred tačke u kojoj se luk trenutno nalazi povećava i to utoliko više ukoliko je snaga luka veća, a brzina njegovog kretanja manja. Slika 1. se odnosi na uslove stacionarnog prenosa toplote. U tim uslovima je razlika u temperaturama ivice žleba i OM, duž šava konstantna, zbog čega je brzina hlađenja ZUT konstantna.

The recommended cooling times $t_{8/5}$, for low-carbon and micro-alloyed steel, which includes steel P 460 NL1, range from 10 to 25 sec. [5], 15 sec [6] and 5 - 20 sec. [7]. Differences in recommended cooling times are the result of differences in chemical composition and microstructure of investigated BM. For the purposes of this paper, as optimal, the cooling time range $t_{8/5}$ of 10 to 20 sec was adopted. Calculated times $t_{8/5}$, table 3, and are at the lower limit of optimal values.

The spread of heat in BM, in arc welding, is shown in figure 1 [8]. The picture shows that the layout of temperatures and shapes of temperature fields change at different forces and speeds of arc moving. It can be seen from the picture that BM temperature on left and right and in front of the point, where arc is currently located, increases, and this is all the more if arc power is larger and movement speed is lower. Figure 1 refers to the conditions of stationary heat transfer. In these conditions, the temperature difference between groove edge and BM is constant; along joint is constant, which is reason for constant cooling rate of HAZ.



Slika 1. Raspored temperatura u OM usled zagrevanja toplotom električnog luka, pri različitim parametrima zavarivanja

Figure 1. Temperature distribution in the BM due to heating by an electric arc, for different welding parameters

Na počecima zavara vladaju nestacionarni uslovi prenosa toplote. Osnovni materijal je hladniji nego na delu spoja gde vladaju stacionarni uslovi. Zbog toga je na počecima zavara brzina hlađenja ZUT veća nego na delovima zavara gde vladaju stacionarni uslovi. Sa povećanjem dužine spoja, toplota luka sve više zagreva OM, zbog čega raste njegova temperatura [3]. Ona, nakon određene dužine spoja, dostiže veličinu koju ima na delu spoja gde vladaju stacionarni uslovi.

At beginning of runs, unsteady conditions of heat transfer are governed. Base material is colder than part of the joint where the stationary conditions prevail. Therefore, at the beginning of runs, HAZ cooling rate is higher than on runs where the stationary conditions prevail. With increasing of joint length, electrical arc is increasingly heats BM, which increases its temperature [3]. It, after a certain joint length, reaches the size equal to the part of joint where the stationary conditions prevail.



Za određivanje uticaja temperature ivice žleba na vreme hlađenja $t_{8/5}$ može se koristiti jednačina (1), pod uslovom da se temperatura predgrevanja T_p zameni temperaturom ivice žleba. Zamena ovih temperatura je moguća s obzirom da T_p , takođe, pretstavlja temperaturu ivica žleba.

Slika 1. pokazuje da su temperature ivice žleba u tački u kojoj se luk trenutno nalazi različite i da zavise od snage luka i brzine zavarivanja. Osim toga ove temperature zavise i od oblika i dimenzija žleba, toplotnih karakteristika OM, odabranog postupka zavarivanja i temperature predgrevanja. Pošto je povećanje temperature ivice žleba, usled zagrevanja toplotom luka teško precizno odrediti, da bi se utvrdilo da li je određeni spoj zavaren pri optimalnim vremenima hlađenja $t_{8/5}$ potrebna su naknadna ispitivanja ZUT, npr. makrostruktura i mikrostruktura ispitivanja, merenja tvrdoća, ispitivanje žilavosti loma.

3. EKSPERIMENT I REZULTATI ISPITIVANJA

Za zavarivanje eksperimentalnog spoja korišćene su ploče dimenzija $500 \times 200 \times 14$ mm od čelika P 460 NL1, tabela 1. Spoj je zavaren MAG postupkom. Korišćen je DM VAC 65 prečnika 1,2 mm, proizvođača "Elektrode Jesenice" i zaštini gas 82% Ar – 18% CO₂ pri protoku od 12 l/min. Karakteristike DM su date u tabelama 4. i 5. Za zavarivanje je korišćen uređaj Kemppi FastMig Pulse 350. Zavarivanje je izvedeno u V žlebu sa uglom otvora 60°, visinom zatupljenja 1 do 2 mm i razmakom u korenu 3 do 4 mm. Uslovi zavarivanja ukrućenih spojeva na konstrukcijama su simulirani zavarivanjem vertikalnih rebara na ploče, čime su u spoju, povećani zaostali naponi, slika 2.

Equation (1) can be used to determine the influence of groove edge temperature on cooling time $t_{8/5}$, provided that the preheating temperature T_p is replaced by groove edge temperature. Replacement of these temperatures is possible since T_p also represents the groove edges temperature. Figure 1 show that groove edges temeperatures at a point of currently electrical arc is different and depend on electrical arc strength and welding speed. In addition, these temperatures also depend on shape and dimensions of groove edge, thermal characteristics of BM, selected welding process and preheating temperature. Since, the increase in the temperature of groove edge is difficult to determine precisely, caused by electrical arc heat, in order to determine whether a particular weld is welded at optimum cooling times $t_{8/5}$, subsequent HAZ tests are required, e.g. macro structural and microstructure tests, hardness measurements, fracture toughness testing.

3. EXPERIMENT AND EXAMINATION RESULTS

Plates of dimension $500 \times 200 \times 14$ mm made of steel P 460 NL1, table 1. were used for welding the experimental joint. The joint was welded with GMAW process. Filler material DM VAC 65 with diameter of 1.2 mm, produced by "Electrodes Jesenice" and protection gas 82% Ar - 18% CO₂ at flow rate of 12 l/min, were used. FM characteristics are given in tables 4 and 5. For the welding, the Kemppi FastMig Pulse 350 was used. The welding was carried out on V groove with angle of 60 °, and root height of 1 to 2 mm and a root gap 3 to 4 mm. The welding conditions of the stiffened joints on the structures were simulated by welding the vertical ribs onto the plates, which resulted in the increased residual stresses, figure 2.

C	Si	Mn	P	S
0,08	1,00	1,70	< 0,025	< 0,025

Table 4. Chemical composition of filler material VAC 65 (%)

Tabela 4. Hemski sastav dodatnog materijala VAC 65 (%)

Yield strength R_p MPa	Tensile strength R_m MPa	Elongation A_5 %	Toughness on - 40°C A_v J
> 460	560 – 690	> 22	> 47

Table 5. Mechanical properties of weld metal of filler material VAC 65
Tabela 5. Mehničke osobine čistog metala šava dodatnog materijala VAC 65

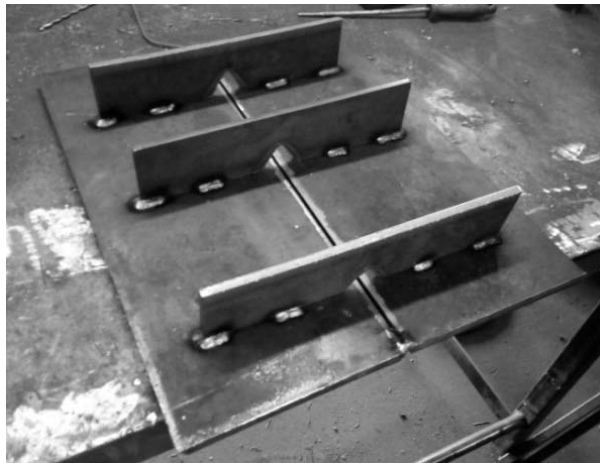


Figure 2. Plate prepared for welding
Slika 2. Ploča pripremljena za zavarivanje

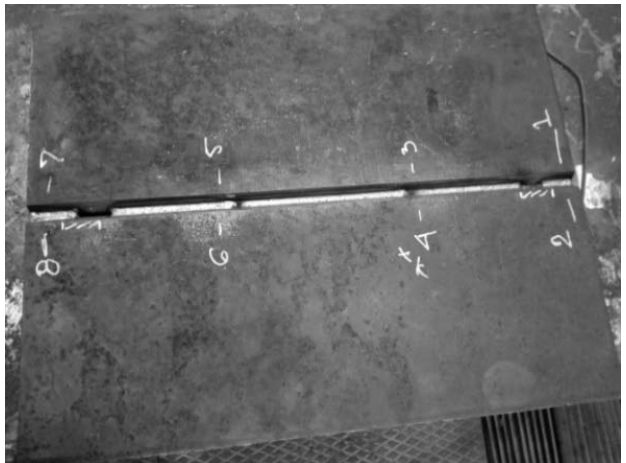


Figure 3. Root run with deliberately made imperfections
Slika 3. Koreni zavar sa namerno napravljenim greškama

Parametri zavarivanja eksperimentalnog spoja su dati u tabeli 6. U korenom zavaru su namerno napravljene greške, neprovareni koren na početku i na kraju spoja, slika 3. Tokom zavarivanja kontinualno su mereni jačina struje i napon pomoću uređaja Kemppi ARC Q, što je omogućilo da se precizno odredi količina unete topline u svakom pojedinačnom zavaru. Slika 4. prikazuje raspored pojedinačnih zavara.

Welding parameters of the experimental joint are given in table 6. At the root run, imperfections were made intentionally, the unfused root at the beginning and at the end of the joint, figure 3. During the welding, the current and voltage were measured continuously with the Kemppi ARC Q, which enabled the precisely determining of heat input in each individual run. Figure 4 shows the schedule of individual runs.

Run	T_p/T_{mp} (°C)	I (A)	U (V)	v_z (mm/sec)	Q (kJ/mm)
Run	50	114	17,8	2,36	0,69
I-Fill	48	171	20,2	3,45	0,80
II-Fill	55	233	27,0	6,02	0,84
III-Fill	59	238	26,7	4,90	1,03
IV-Fill	60	237	26,2	4,24	1,17
V-Fill	50	238	25,8	4,53	1,08

Table 6. Welding parameters and the heat input of the experimental joint
Tabela 6. Parametri zavarivanja i količine unete topline eksperimentalnog spoja

Tokom zavarivanja svakog zavara merene su temperature OM pored ivica žleba u tačkama 1 do 8, slika 3. Temperature su merene IC termometrom, koji je prethodno baždaren pomoću kontaktnega termometra. Iz spoja su, za ispitivanja, uzeta dva uzorka, uzorak 1. u blizini početka spoja i uzorak 2. u blizini kraja spoja, slika 5. Temperature ivica žleba na površinama ispitnih uzoraka su određene aproksimacijom pomoću temperatura izmerenih u tačkama između kojih se uzorak nalazi.

During the welding of each run, the BM temperatures were measured along the groove edges in points 1 to 8, fig. 3. The temperatures were measured with an IC thermometer, which was previously calibrated using a contact thermometer. From the joint, for testing, were taken two samples, sample 1, near the beginning of the joint and sample 2, near the end of the joint, figure 5. The groove edges temperatures on the test sample surfaces was determined by approximation using the temperature measured at the points between which the sample is located.

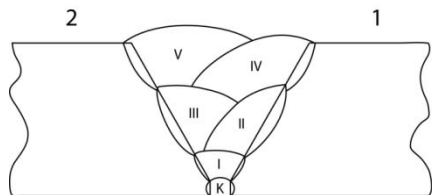


Figure 4. Welding schedule
Slika 4. Raspored zavara

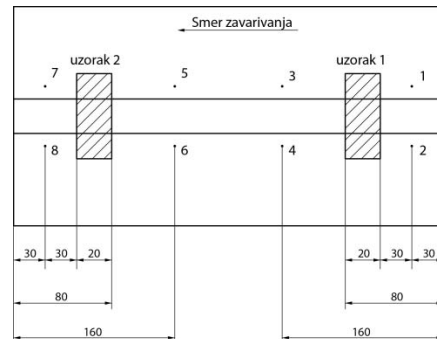


Figure 5. Samples location 1 and 2
Slika 5. Mesta uzimanja uzoraka 1. i 2.

U tabeli 7. su, za oba uzorka, date temperature ivica žleba za pojedinačne zavare, količine unete toplote i na osnovu njih izračunata vremena $t_{8/5}$ u ZUT svakog pojedinačnog zavara.

In table 7, for each sample, the groove edges temperatures for the individual runs, heat input and the basis of them calculated the time $t_{8/5}$ in the HAZ of each individual run is given.

Run	Sample 1.			Sample 2.		
	T (°C)	Q (kJ/mm)	$t_{8/5}$ (sec.)	T (°C)	Q (kJ/mm)	$t_{8/5}$ (sec.)
Root	94	0,69	3,4	188	0,69	5,8
Fill I	105	0,80	4,9	178	0,80	7,4
Fill II	113	0,84	5,6	234	0,84	11,8
Fill III	112	1,03	8,4	269	1,03	23,3
Fill IV	110	1,17	10,8	230	1,17	22,2
Fill V	110	1,08	9,2	230	1,08	19,0

Table 7. Groove edges temperatures and the cooling times $t_{8/5}$ near start and end of joint
Tabela 7. Temperatura ivica žleba i vremena hlađenja $t_{8/5}$ u blizini početka i kraja spoja

Slike 6. i 7. prikazuju makrostrukture uzoraka 1. i 2. Uzorci za ispitivanje makrostruktura su pripremljeni brušenjem, a zatim su nagriženi u 3% rastvoru Nitala. Na obe slike se uočavaju greške i to, na slici 6. neprovareni koren, a na slici 7. pora u WM uz liniju stapanja.

Figures 6 and 7 show the macrostructure of samples 1 and 2. The samples for macrostructure testing were prepared by grinding and then etched by 3% Nital solution. In both pictures, imperfections are noticed, and in figure 6, the unfused root, and in figure 7, the pore in the WM near the fusion line.

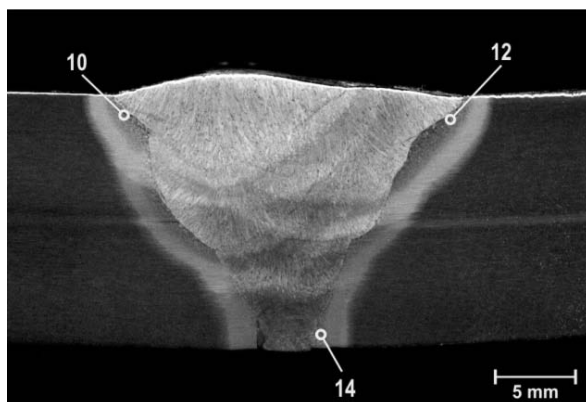


Figure 6. Macrostructure of sample 1.
Slika 6. Makrostruktura uzorka 1.

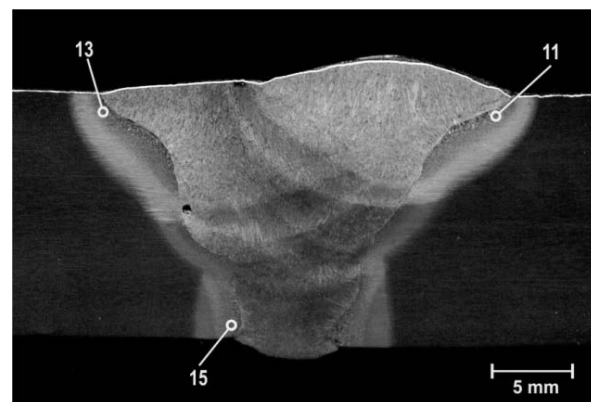


Figure 7. Macrostructure of sample 2.
Slika 7. Makrostruktura uzorka 2.



Sa slike se vidi i da je širina MŠ uzorka 2. veća od širine MŠ uzorka 1. Ovo je naročito izraženo u zoni korena spoja, gde se razlike u širinama MŠ kreću od 1,2 do 2,2 mm (30 do 50%) i lica spoja, gde se te razlike kreću od 1,8 do 3,8 mm (10 do 20%). Razlike u širinama MŠ na sredini spoja su manje i kreću se do 0,5 mm.

Slike pokazuju i da je širina ZUT uzorka 2. veća od širine ZUT uzorka 1. U korenom delu spoja razlika u širinama ZUT se kreće od 1,6 do 3,0 mm (60 do 100%), a u zoni lica spoja ta razlika se kreće od 1,8 do 2,4 mm (30 do 45%). Razlike u širinama ZUT oba uzorka su minimalne u sredini spoja. Sa slike se vidi i da je ZUT završnih zavara, na oba uzorka uži na površini OM nego ispod njegove površine. Širina ZUT završnih zavara je najveća na dubini 2 do 4 mm ispod površine OM. Slike pokazuju da se grubozrni ZUT, u uzorku 1., pojavljuje u ZUT završnih zavara, a u uzorku 2. i u ZUT završnih zavara i u ZUT korenog zavara. Grubozrne zone u uzorku 1. su uže, zahvataju manju površinu i prostiru se na dubini 1 do 2,5 mm. U uzorku 2. grubozrne zone uz lice spoja su šire, zahvataju veću površinu i prostiru se na dubini od 1 do 4 mm. U ZUT korenog zavara 2. grubozrni ZUT se prostire do dubine od 1 mm.

Tvrdoće su izmerene metodom Vickers, silom utiskivanja od 49N (HV5), na uređaju "Wolpert Dijatestor 2RC" [9]. Tvrdoće OM, u oba uzorka, se kreću između 190 i 210 HV 5. Tvrdoće u MŠ uzorka 1. u zoni lica spoja iznose 232 HV5, a u zoni korena spoja 210 HV5. Tvrdoće MŠ uzorka 2. se kreću između 232 i 257 HV5 u zoni lica spoja i oko 232 HV5 u zoni korena spoja. Tvrdoće u ZUT su date u tabelama 8. i 9. Zatamnjene cifre pretstavljaju tvrdoće izmerene na linijama stapanja ili u njihovoj neposrednoj blizini u ZUT. Na slikama 8. i 9. prikazan je raspored mesta merenja tvrdoća u ZUT oba uzorka.

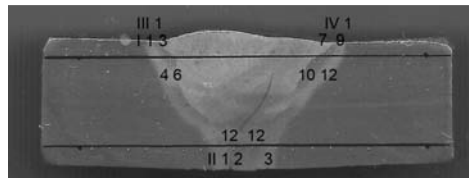


Figure 8. Schedule of hardness measuring point 1
Slika 8. Raspored mesta merenja tvrdoća 1.

The picture shows that the width of the WM of the sample 2 is larger than the width of the WM of sample 1. This is especially expressed in the root zone of the joint, where the differences in the widths of the WM range from 1.2 to 2.2 mm (30 to 50%) and joint faces, where these differences range from 1.8 to 3.8 mm (10 to 20%). The differences in the widths of the WM in the middle of the joint are smaller and range up to 0.5 mm. The pictures also show that the width of the HAZ of the sample 2 is greater than the sample 1. At the root of the joint, the difference in the widths of the HAZ ranges from 1.6 to 3.0 mm (60 to 100%), and in the face joint, the difference is ranges from 1.8 to 2.4 mm (30 to 45%). The differences in the widths of the HAZ are both minimal in the middle of the joint. From the pictures it can be seen that the HAZ of the final runs, on both samples, is narrower on the surface of the BM, than below its surface. The width of the final runs HAZ is the largest at a depth of 2 to 4 mm below the BM surface. The images show that coarse-grained HAZ, in sample 1, appears in HAZ of final runs, and in sample 2 it appears in final runs HAZ and in root runs HAZ, also. The coarse zones in the sample 1 are narrow; they engage in a smaller surface and extend at a depth of 1 to 2.5 mm. In the sample of the coarse-grained zone 2, the joints are wider; they cover a larger surface and extend at a depth of 1 to 4 mm. In the roots HAZ of the sample 2 coarse HAZ extends to a depth of 1 mm. The hardness was measured by the Vickers method, by injection force of 49N (HV5) on the "Wolpert Dijatestor 2RC" [9]. The hardness of the BM in both samples ranges between 190 and 210 HV 5. The hardness in the WM of sample 1. In the face zone of joint is 232 HV5, and in the root zone of the joint is 210 HV5. The WM hardness of the sample 2. ranges between 232 and 257 HV5 in the face zone and about 232 HV5 in the root zone of the joint. Hardness in HAZ is given in tables 8 and 9. Dimming digits represent the hardness measured on the fusion lines or in their immediate vicinity in the HAZ. Figures 8 and 9 shows the layout of the hardness measurement point in the HAZ of both samples.

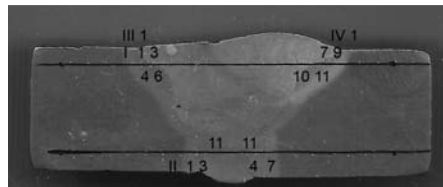


Figure 9. Schedule of hardness measuring point 2
Slika 9. Raspored mesta merenja tvrdoća 2.



	1	2	3	4	5	6	7	8	9	10	11	12
I	257	313	353	257	328	286	336	353	262	371	345	321
II	257	257	321									
III	353	362	321	286	321	286	321	286	321	257	286	257
IV	321	362	362	362	321	286	362	286	286	257	286	321

*Table 8. HAZ sample 1. Hardness measurement results (HV 5)**Tabela 8. Rezultati merenja tvrdoća u ZUT uzorka 1. (HV 5)*

	1	2	3	4	5	6	7	8	9	10	11
I	274	313	293	290	321	358	299	366	345	362	386
II	257	286	286	257	286	286	232				
III	293	358	321	321	286	257	286	286	257	257	286
IV	336	362	362	321	286	286	286	210	286	257	257

*Table 9. HAZ sample 2. Hardness measurement results (HV 5)**Tabela 9. Rezultati merenja tvrdoća u ZUT uzorka 2. (HV 5)*

Sa slike i iz tabele se vidi da su, na oba uzorka, maksimalne vrednosti tvrdoća izmerene u ZUT završnih zavara (362 HV 5) i da tvrdoće ZUT opadaju od lica ka korenju spoja (362 do 260 – 280 HV 5). Ove vrednosti su praktično iste u oba uzorka.

Slike 10. do 15. prikazuju mikrostrukture u ZUT oba uzorka, koje su reprezentativne za temu ovog rada. Mikrostrukture su pregledane na metalografskom mikroskopu "Letiz" i ovde su prikazana karakteristična mesta [10]. Pozicija svakog karakterističnog mesta je označena na odgovarajućoj makrofotografiji, slike 6. i 7. Mikrostrukture su otkrivene nagrizanjem u 5% rastvoru Nitala.

With the figures and from the table it can be seen that the maximum hardness values were measured in the HAZ of the final runs (362 HV 5) on both samples and that the HAZ hardness dropped from the face to the root of the joint (362 to 260 – 280 HV 5). These values are practically the same in both samples. Figures 10 through 15 show the microstructures in the HAZ of both samples, which are representative of the subject of this paper. The microstructures were examined on the metallographic microscope "Letiz", and characteristic sites are shown [10]. The position of each characteristic spot is indicated on the appropriate macrophotography, figures 6 and 7. Microstructures were detected by etching in a 5% Nital solution.

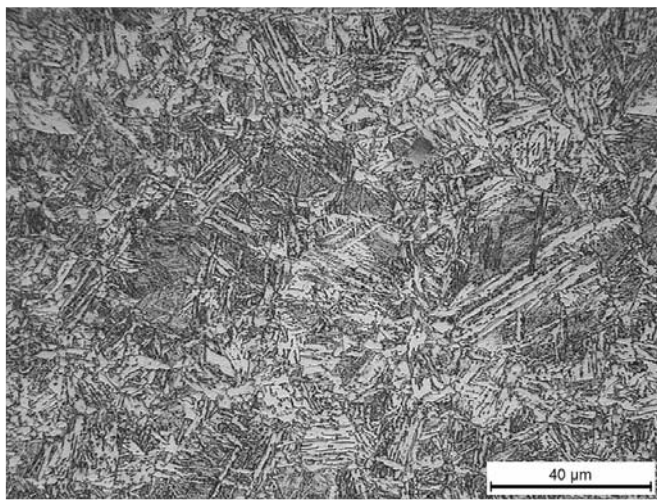


Figure 10. Sample 1, face of joint, HAZ of last run, upper bainite

Slika 10. Uzorak 1., lice spoja, ZUT poslednjeg zavara, gornji beinit

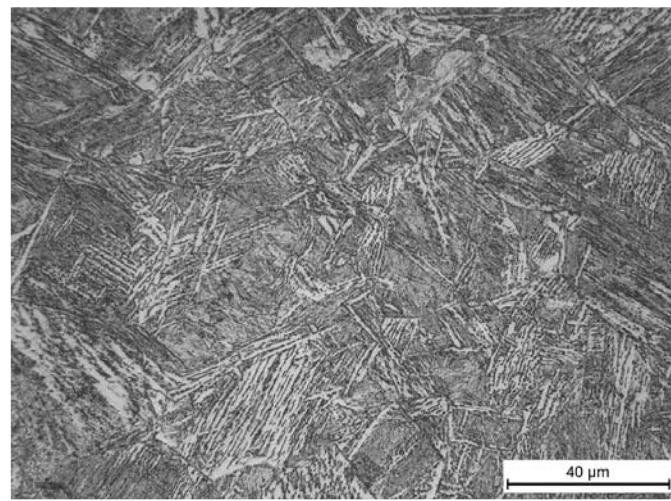
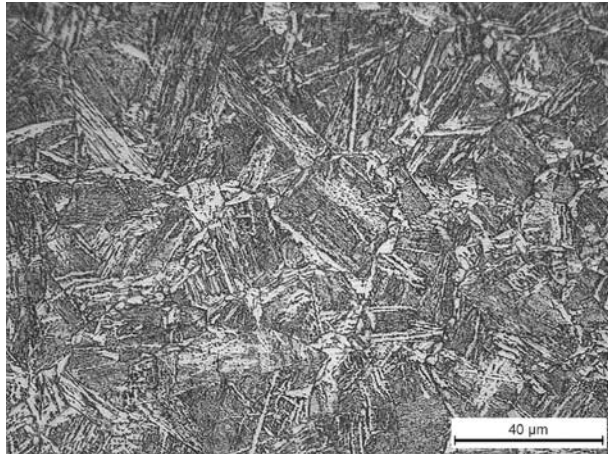


Figure 11. Sample 2, face of joint, HAZ of last run, upper bainite

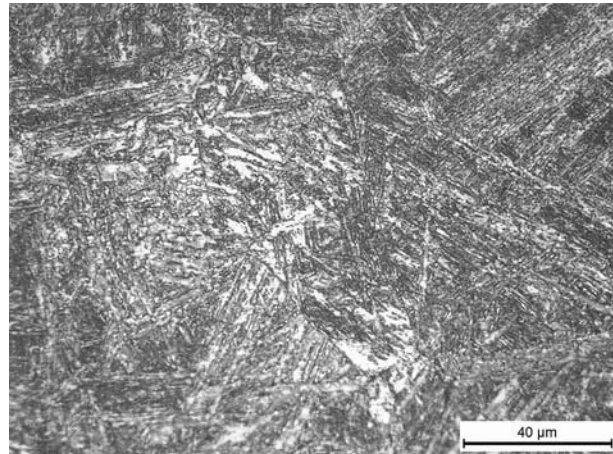
Slika 11. Uzorak 2., lice spoja, ZUT poslednjeg zavara, gornji beinit



500 X

Figure 12. Sample 1. face of joint, HAZ of before last run, upper bainite

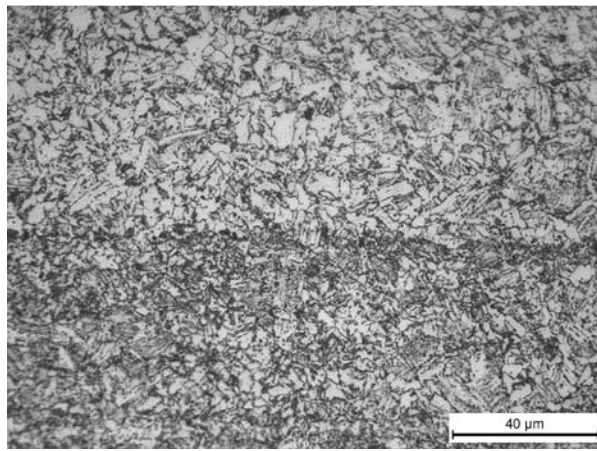
Slika 12. Uzorak 1. lice spoja, ZUT pretposlednjeg zavara, gornji beinit



500 X

Figure 13. Sample 2. face of joint, HAZ of before last run, upper bainite

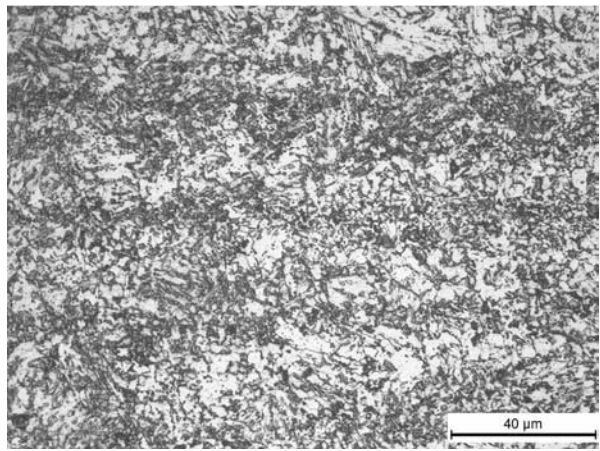
Slika 13. Uzorak 2. lice spoja, ZUT pretposlednjeg zavara, gornji beinit



500 X

Figure 14. Sample 1., HAZ of root run, grain bainite

Slika 14. Uzorak 1., ZUT korenog zavara, zrnasti beinit



500 X

Figure 15. Sample 2., HAZ of root run, grain bainite

Slika 15. Uzorak 2., ZUT korenog zavara, zrnasti beinit

Slike 10. do 13. prikazuju mikrostrukture grubozrnih delova ZUT završnih zavara tj. zavara lica spoja. Kod oba uzorka mikrostrukture su beinitne (gornji beinit). Mikrostruktura uzorka 2. je grubozrnija i u njoj je uočeno prisustvo Widmannstattenovog ferita. Slike 14. i 15. prikazuju mikrostrukture u korenom delu ZUT. Kod oba uzorka mikrostrukture su beinitne (zrnasti beinit).

4. ANALIZA REZULTATA

Svi zavari su zavareni pri praktično istoj polaznoj temperaturi, tabela 6. Vrednosti iz tabele 7. pokazuju da temperature ivica žleba duž spoja rastu. Temperaturе ivica žleba, pri zavarivanju pojedinih zavara kod uzorka 1., su ujednačene i kreću se oko 110°C. Kod uzorka 2. temperature ivica žleba su znatno više i neujednačenije. Tabele pokazuju da je na prvih 80 mm spoja temperatura

Figs. 10 through 13 depict the microstructures of the coarse-grained portions of the final runs HAZ, i.e. the face runs of the joint. In both samples, microstructures are bainite (upper bainite). The microstructure of the sample 2 is cruder and shows the presence of the Widmannstatten ferrite. Figures 14 and 15 show the microstructures at the root of the HAZ. In both samples, the microstructure is bainite (grain bainite).

4. ANALYSIS OF RESULTS

All welds are welded at practically the same starting temperature, table 6. The values in table 7. show that the temperatures of the groove edges along the joint increase. The groove edges temperatures, when welding the individual runs in the sample 1, are uniform and range around 110°C. For the sample 2, the temperature groove edges are considerably higher and more uneven. Tables show that on the first 80 mm of the joint, the groove edge



ivice žleba rasla prosečno za 50 do 60 °C. Na daljih 340 mm spoja temperatura ivice žleba, pri zavarivanju pojedinih zavara, je rasla od 2 do 2,5 puta. U odnosu na početke pojedinih zavara temperature ivice žleba uzorka 2. su veće od 3,8 do 4,5 puta.

Vrednosti iz tabele 7. pokazuju da su vremena hlađenja $t_{8/5}$ u uzorku 1. uglavnom manja u odnosu na donju usvojenu vrednost za vreme $t_{8/5}$ za čelik P 460 NL1. Samo u završnim zavarima vremena $t_{8/5}$ su bliska donjoj usvojenoj vrednosti. U uzorku 2. vremena hlađenja $t_{8/5}$ su u prvim prolazima manja od donje usvojene vrednosti, a u završnim zavarima su veća od gornje usvojene vrednosti za ovaj čelik. Da bi se vreme $t_{8/5}$ održalo u usvojenim granicama potrebne su korekcije temperature predgrevanja i količina unete toplote za koren zavar i prvi zavar popune i ograničenje maksimalne temperature ivice žleba.

Slike 6. i 7. pokazuju da su širine MŠ i ZUT u uzorku 2. veće nego u uzorku 1. Ovo je posledica viših temperatura ivica žleba i sporijeg hlađenja u ovom delu spoja. Pri konstantnoj količini unete toplote usporavanje hlađenja ima za posledicu povećanje dubine topanja OM i time i povećanje dimenzija MŠ i ZUT. Ovo ima za posledicu i povećanje stepena mešanja OM i DM zbog čega se povećava udio OM u sastavu MŠ [3]. Povećanje širine MŠ i ZUT je najveće u korenom delu spoja. I pored najmanjeg unosa toplote i najnižih temperatura ivica žleba dubina uvarivanja, u ovom delu spoja, je najveća zbog najmanje mase OM koja se zagreva toplotom luka pri zavarivanju korenog i prvog zavara popune, što je uslovljeno V oblikom žleba. Povećanja širina MŠ i ZUT su nešto manja u zoni lica spoja, a najmanja su u sredini spoja. Veće širine MŠ i ZUT u zoni lica spoja, u odnosu na sredinu spoja, su posledica većih unosa toplote i većih jačina struje pri zavarivanju poslednjih zavara.

Zone sa grubozrnom strukturom u ZUT su uočene na oba uzorka. U uzorku 1. ove zone se javljaju u ZUT završnih zavara, a u uzorku 2. i u ZUT završnih zavara i u ZUT korenih zavara. Grubožrne zone u uzorku 1. su uže, zahvataju manju površinu i prostiru se na manjoj dubini nego grubozrne zone u završnim zavarima uzorka 2. Pojava grubozrnh zona u ZUT korenog zavara uzorka 2., i veće dimenzije i krupnije zrno u grubozrnm zonama uz lice spoja ovog uzorka su posledica njegovog sporijeg hlađenja, odnosno viših temperatura ivica žleba.

Imajući u vidu heterogenost struktura ZUT [11], verovatnoća otkrivanja delova ZUT malih zapremina sa drugačijom strukturom u odnosu na

temperature increased by an average of 50 to 60 °C. On a further 340 mm of joint, the groove edge temperature, when welding individual runs, increased from 2 to 2.5 times. In relation to the beginnings of individual runs, the groove edge temperature of the sample 2 is greater than 3.8 to 4.5 times. The values in Table 7 show that cooling times $t_{8/5}$ in sample 1, are generally lower in relation to the lower value of adopted cooling time $t_{8/5}$ for steel P 460 NL1. Only in the end runs, cooling times $t_{8/5}$ are close to the lower accepted value. In the sample 2, cooling times $t_{8/5}$ in the first passes is lower than the adopted lower value, and in the final runs, they are higher than the upper values adopted for this steel. In order to keep the cooling time $t_{8/5}$ within the adopted limits, corrections of the preheating temperature and the heat input for the root run and the first filling run and limiting the maximum groove edge temperature is required. Figures 6 and 7 show that the widths of WM and HAZ in sample 2 are higher than in sample 1. This is due to higher groove edges temperatures and slower cooling in this part of the joint. With a constant heat input, the slowing down of cooling, results in an increase in the fusion depth of the BM and consequently an increase in the dimensions of the WM and HAZ. This also results in an increase in the degree of mixing of BM and FM, which increases the proportion of BM in the composition of the WM [3]. Increasing the width of the WM and HAZ is the largest in the root part of the joint. Despite the smallest heat input and the lowest groove edges temperatures, the depth of penetration in this part of the joint, is the greatest, because of the lowest mass of the BM which is heated by the arc during the welding of the root and the first filling run, which is conditioned in the shape of the groove. Increases in the width of the WM and HAZ are somewhat smaller in the face zone, and the smallest in the middle of the joint. The larger width of the WM and the HAZ in the face zone, in relation to the center of the joint, are due to higher heat inputs and higher current intensities in the welding of the last runs. Coarse-grained HAZ zones were observed on both samples. In sample 1, these zones appear in HAZ of final runs, and in sample 2, in HAZ of final runs and in HAZ root runs. The coarse-grained zones in the sample 1. are narrow, engage in a smaller surface and extend at a lower depth than the coarse-grained zone in the final runs of the sample 2. The appearance of coarse-grained zones in the HAZ root runs of sample 2, and larger dimensions and bigger grains in coarse-grain zones along the face of the joint of this sample, are due to



okolinu se povećava sa smanjenjem dimenzija otiska tj. sa smanjenjem opterećenja. Zbog toga su u ovom slučaju tvrdoće merene metodom Vickers malom silom utiskivanja. Ovo omogućava i povećanje učestalosti merenja što dalje povećava verovatnoću otkrivanja malih delova ZUT sa drugačijom strukturom. U oba uzorka tvrdoće su merene po linijama stapanja i u njihovoј blizini. Najveće tvrdoće (362 HV5) su izmerene u ZUT završnih zavara, u njihovim grubozrnim zonama. Idući ka korenu spoja, na oba uzorka, tvrdoće opadaju do istog nivoa (260 – 280 HV5).

Maksimalne izmerene tvrdoće, na oba uzorka, su nešto veće od maksimalne prihvatljive tvrdoće (350 HV) za nikougljenične i mikrolegirane čelike. Pri tvrdoćama većim od 350 HV, kod ovih čelika, se povećava sklonost ZUT ka pojavi hladnih prslina [2, 3]. Iz rezultata ispitivanja se vidi da promena temperature ivice žleba nije izazvala promenu u veličini maksimalne tvrdoće u ZUT, ali jeste izazvala promenu u raspodeli tvrdoća. Rezultati merenja pokazuju da su tvrdoće MŠ uzorka 2. nešto veće od tvrdoća MŠ uzorka 1. i u zoni lica i u zoni korena spoja. Prethodna razmatranja pokazuju da se u uzorku 2. može očekivati veći udeo OM u MŠ nego u uzorku 1. S obzirom da OM ima viši sadržaj C, tabela 1. u odnosu na DM, tabela 4. može se očekivati da se u MŠ uzorka 2. poveća sadržaj C što je kod niskougljeničnog MŠ praćeno povećanjem tvrdoće.

Najveća pažnja pri ispitivanju mikrostruktura je posvećena delovima ZUT uz linije stapanja. U oba uzorka, u ovim delovima ZUT struktura je grubozrna i čini je beinit. Najgrublje mikrostrukture se javljaju u blizini lica spoja, u ZUT završnih zavara. Idući ka korenu spoja oblik beinita se menja iz igličastog u zrnasti, što je posledica višestepenog otpuštanja [12]. U oba uzorka mikrostruktura se, idući od lica ka korenu spoja, menja na isti način. U grubozrnom delu ZUT uz lice spoja uzorka 2. struktura grublja, što je posledica sporijeg hlađenja. Mikrostrukturalna ispitivanja pokazuju da bitnih razlika u mikrostrukturama oba uzorka nema. Ovo potvrđuju i rezultati merenja tvrdoća.

its slower cooling, or higher groove edges temperatures. Bearing in mind the heterogeneity of the HAZ structure [11], the probability of detecting parts of HAZ of small volumes with a different structure in relation to the environment increases with decreasing the size of the indentation, with reduced load. Therefore, in this case, the hardness was measured by the Vickers method with a small force of imprinting. This also allows increasing the frequency of measurement, which further increases the probability of detecting small parts of the HAZ with a different structure. Both hardness patterns were measured along the merging lines and in their vicinity. The highest hardness (362 HV5) was measured in the HAZ end runs, in their coarse zones. Further to the root of the joint, on both samples, the hardness decreases to the same level (260 - 280 HV5). The maximum measured hardness, on both samples, is slightly higher than the maximum acceptable hardness (350 HV) for low-carbon and micro-alloyed steels. For hardness greater than 350 HV, in these steels, the inclination of HAZ to appearance of cold cracks increases [2, 3]. From the results of the test, it can be seen that the change in the groove edge temperature did not cause a change in the value of the maximum hardness of HAZ, but it caused a change in the distribution of the hardness. The results of the measurement show that the hardness of the WM of the sample 2 is slightly higher than the hardness of the WM of the sample 1. both in the face zone and in the root zone of the joint. Preliminary considerations show that in sample 2. a higher proportion of BM in the WM can be expected than in sample 1. Since BM has higher content C, table 1 in relation to FM, table 4, can be expected to increase the content of C be in sample 2, which is accompanied by a hardness increasing in the low-carbon WM. The greatest attention in the microstructure testing is dedicated to the HAZ parts along the fusion line. In both samples, in these parts of the HAZ, the structure is rough and makes it bainite. The roughest microstructures occur near the face of the joint, in the HAZ end runs. Next to the root of the joint, the shape of the bainite changes from the needle to the grains, which is the consequence of the multistage annealing[12]? In both samples, the microstructure changes, in the same way, from the face to the root of the joint. In the coarse part of the HAZ, on the joint face of the sample, structure is rougher, which is a consequence of slower cooling. Microstructural testing shows that there are no significant differences in the microstructures of both samples. This is confirmed by the results of hardness measuremen



5. Zaključci

Temperatura ivica žleba raste tokom zavarivanja zbog zagrevanja osnovnog materijala topotom luka. Porast temperature ivice žleba usporava hlađenje zone uticaja toplote i produžava vreme hlađenja $t_{8/5}$. Pri izradi tehnologija zavarivanja, naročito za čelike visokih čvrstoća, potrebno je definisati minimalno i maksimalno vreme hlađenja $t_{8/5}$ tj. potrebno je definisati dijapazon vrednosti u kojima se vreme hlađenja $t_{8/5}$ može kretati.

Ispitivanje makrostruktura pokazuje da se širine metala šava i zone uticaja toplote, duž spoja povećavaju. Povećanje dimenzija metala šava i zone uticaja toplote su posledica usporavanja hlađenja zbog povećanja temperatura ivica žleba duž spoja. Usporavanje hlađenja ima za posledicu i povećanje dimenzija grubozrnog dela zone uticaja toplote.

Rezultati merenja tvrdoča pokazuju da promena temperatura ivica žleba, duž spoja, nije uticala na promenu maksimalne vrednosti tvrdoče u zoni uticaja toplote. Najveće tvrdoče su izmerene u grubozrnim zonama završnih zavara i one su bliske maksimalnim prihvativim vrednostima za niskougljenične i mikroleđigirane čelike.

Ispitivanjem mikrostruktura, u zoni uticaja toplote, nisu otkrivene razlike u strukturama izazvane promenom vremena hlađenja $t_{8/5}$ duž spoja. Pri svim vremenima hlađenja u grubozrnom delu zone uticaja toplote se javlja beinit. Promena vremena hlađenja je uticala samo na krupnoču strukture, tako da je pri manjim brzinama hlađenja dobijen grubozrnji beinit.

Ovaj rad je proistekao iz rezultata istraživanja na projektu broj TR 35024, finansiranog od strane Ministarstva prosvete, nauke i tehnološkog razvoja Republike Srbije.

Literature

- [1] I. Hrvnjak: *Zavarljivost čelika*, Građevinska knjiga, Beograd, 1982.
- [2] A. Radović: *Zavarljivost i ispitivanje zavarljivosti*, Monografija Mehanika loma zavarenih spojeva, Goša Institut, Tehnološko metalurški fakultet Beograd, Beograd, 1985.
- [3] H. Granjon: *Metalurške osnove varjenja*, prevod na slovenački P. Štular, Zveza društev za varilno tehniko Slovenije, Ljubljana, 1994.
- [4] R. Jovičić: Metode za izračunavanje temperaturne predgrevanja pri zavarivanju čelika povišene i visoke čvrstoće, časopis Zavarivanje i zavarene konstrukcije, Vol 61, No 3 (2016), str. 113-119, Publisher: Serbian Welding Society, 2016.
- [5] Standard EN 1011 – 2/2007: *Zavarivanje – Preporuke za zavarivanje metalnih materijala – Deo 2: Elektrolučno zavarivanje feritnih čelika*
- [6] K. Gerić: *Prsline u zavarenim spojevima*, Monografija, Fakultet tehničkih nauka, Novi Sad, 2005.
- [7] Ruukki: *Hot rolled steel sheets, plates and coils, Welding general*, Ruukki Metals Oy, Finland, 2014.
- [8] A. Sedmak i dr.: *Mašinski materijali*, II deo, Univerzitet u Beogradu Mašinski fakultet, Beograd, 2000.
- [9] SRPS EN ISO 6507-1/2011: *Metalni materijali - Ispitivanje tvrdoče po Vikersu - Deo 1: Metoda ispitivanja*
- [10] SRPS EN 1321/2007: *Ispitivanja metodama sa razaranjem zavarenih spojeva metalnih materijala - Makroskopsko i mikroskopsko ispitivanje zavarenih spojeva*
- [11] K. Easterling: *Introduction to the Physical Metallurgy of Welding*, Butterworths Monographs in Metals, UK, 1983.
- [12] H.K.D.K. Bhadeshia, *Steels, Microstructure and properties*, Butterworth Heinemann, Elsevier, Third edition, 2006.